Institute of Space and Aeronautical Science, University of Tokyo
Report No. 466, June 1971

Measurement of Structural Vibrations excited by Random Force

By

Nobuharu AOSHIMA

Summary: Structural vibrations excited by pressure loading which is random in space and time are considered. Power spectra of generalized force and generalized coordinate variables are discussed in general linear vibrating systems. Vibration magnitude of generalized coordinate variables and mode shapes are determined from simultaneous measurement of vibration quantities at many points by summing up the results with variable weightings. As an example, flexural vibration of thin beam, which is acted upon by pressure fluctuation of air flow or random sound pressure, is measured by strain gages and real time spectrum analyzer.

1. Vibration Mode, Generalized Coordinate and Generalized Force

Structural vibrations excited by random force are considered. Vibration system is assumed to be linear and displacement $\xi(\boldsymbol{r}, t)$ is assumed to satisfy next equation.

$$L[\xi(\boldsymbol{r}, t)]+b\frac{\partial\xi(\boldsymbol{r}, t)}{\partial t}+\frac{1}{c^2}\frac{\partial^2}{\partial t^2}\xi(\boldsymbol{r}, t)=p(\boldsymbol{r}, t) \qquad (1)$$

where b and c are constants, $\boldsymbol{r}$ is a position vector, $p(\boldsymbol{r}, t)$ is random load and $L[\ ]$ is a linear differential operator which is self-adjoint and positive definite. The boundary conditions are assumed to be homogeneous. Then the eigenfunctions $y_s(\boldsymbol{r})$ of next equation are orthogonal

$$L[y(\boldsymbol{r})]-\frac{\omega^2}{c^2}y(\boldsymbol{r})=0 \qquad (2)$$

and solution of (1) is written as [*1*]

$$\xi(\boldsymbol{r}, t)=\sum_s q_s(t)y_s(\boldsymbol{r}). \qquad (3)$$

These are general considerations and in the following, attention is focused to bending vibration of thin structure in which $L[\ ]$ is a fourth-order differential operator. Since $\xi(\boldsymbol{r}, t)$ represents vertical displacement of surface point $\boldsymbol{r}$, the work done by pressure load can be expressed as

$$\delta w = \int \delta\xi(\boldsymbol{r}, t)p(\boldsymbol{r}, t)dA = \int \left\{\sum_s \delta q_s(t)y_s(\boldsymbol{r})\right\} p(\boldsymbol{r}, t)dA$$
$$= \sum_s \int \delta q_s(t)y_s(\boldsymbol{r})p(\boldsymbol{r}, t)dA = \sum_s \delta q_s(t)L_s(t) \tag{4}$$

where

$$L_s(t) = \int y_s(\boldsymbol{r})p(\boldsymbol{r}, t)dA, \tag{5}$$

dA is surface element and integration is taken for all over the surface. Right hand of (4) is the sum of works done to each mode, and each work is the multiple of $q_s(t)$ and $L_s(t)$. $q_s(t)$ represents the magnitude of mode $y_s(\boldsymbol{r})$ and can be thought as one kind of displacement variable. Then $L_s(t)$ can be regarded as one kind of force, since it is a conjugate variable of $q_s(t)$. Actually $q_s(t)$ and $L_s(t)$ are known as generalized coordinate and generalized force [2]. Since $p(\boldsymbol{r}, t)$ is random, $q_s(t)$ and $L_s(t)$ are also random, and it is the purpose of this paper to discuss the power spectra of them.

On the other hand, vibration magnitude of the structure as a whole would be expressed by

$$V(f) = \int \Phi_\xi(\boldsymbol{r}, f)dA \tag{6}$$

where

$$\Phi_\xi(\boldsymbol{r}, f) = \int_{-\infty}^{\infty} \overline{\xi(\boldsymbol{r}, t)\xi(\boldsymbol{r}, t+\tau)} \cos 2\pi f\tau d\tau \tag{7}$$

is power spectrum of displacement $\xi(\boldsymbol{r}, t)$. Then $V(f)$ is calculated as

$$V(f) = \int\int_{-\infty}^{\infty} \overline{\sum_s q_s(t)y_s(\boldsymbol{r}) \sum_{s'} q_{s'}(t+\tau)y_{s'}(\boldsymbol{r})} \cos 2\pi f\tau d\tau dA$$
$$= \int_{-\infty}^{\infty} \sum_s \sum_{s'} \left\{\overline{q_s(t)q_{s'}(t+\tau)} \int y_s(\boldsymbol{r})y_{s'}(\boldsymbol{r})dA\right\} \cos 2\pi f\tau d\tau$$
$$= \int_{-\infty}^{\infty} \sum_s \overline{q_s(t)q_s(t+\tau)} \cos 2\pi f\tau d\tau \tag{8}$$
$$= \sum_s \Phi_{q_s}(f)$$

In this deduction, orthonormality of eigenfunctions is used. (8) represents that vibration magnitude $V(f)$ as defined by (6) is the sum of power spectra of generalized coordinates which are written as follows.

$$\Phi_{q_s}(f) = \frac{\Phi_{L_s}(f)}{|Z_s(f)|^2} \tag{9}$$

Where $\Phi_{L_s}(f)$ is the power spectrum of the generalized force and $Z_s(f)$ is the gener-

alized impedance of the system. These quantities are discussed in the following articles.

2. Power Spectrum of Generalized Force

Power spectrum of $L_s(t)$ is calculated as follows.

$$\begin{aligned}\Phi_{L_s}(f) &= \int_{-\infty}^{\infty} \overline{L_s(t)L_s(t+\tau)} \cos 2\pi f\tau d\tau \\ &= \int_{-\infty}^{\infty} \overline{\int y_s(\boldsymbol{r})p(\boldsymbol{r}, t)dA \int y_s(\boldsymbol{r}')p(\boldsymbol{r}', t+\tau)dA'} \cos 2\pi f\tau d\tau \\ &= \int_{-\infty}^{\infty} \int\int \overline{p(\boldsymbol{r}, t)p(\boldsymbol{r}', t+\tau)} y_s(\boldsymbol{r})y_s(\boldsymbol{r}')dAdA' \cos 2\pi f\tau d\tau \\ &= \int\int C(f, \boldsymbol{r}, \boldsymbol{r}')y_s(\boldsymbol{r})y_s(\boldsymbol{r}')dAdA'\end{aligned} \tag{10}$$

where

$$\begin{aligned}C(f, \boldsymbol{r}, \boldsymbol{r}') &= \int_{-\infty}^{\infty} \overline{p(\boldsymbol{r}, t)p(\boldsymbol{r}', t+\tau)} \cos 2\pi f\tau d\tau \\ &= \mathscr{R}e\{\Phi_{pp'}(f)\}\end{aligned} \tag{11}$$

is the real part of the cross power spectrum of pressure loads at two points $\boldsymbol{r}$ and $\boldsymbol{r}'$.

As an example of $C(f, \boldsymbol{r}, \boldsymbol{r}')$, a number of point sound sources which are distributed randomly are considered. From the n-th source, sound travels to two detection points with delay time τ_n, τ_n' and strength a_n, a_n'. Then sound pressures at two points are

$$p_1(t) = \sum_n a_n S_n(t-\tau_n), \qquad p_2(t) = \sum_n a_n' S_n(t-\tau_n') \tag{12}$$

$S_n(t)$ is the n-th source function and when $n \neq n'$, it is assumed that $S_n(t)$ is uncorrelated with $S_{n'}(t)$. Then cross-correlation function of $p_1(t)$ and $p_2(t)$ is

$$\begin{aligned}\overline{p_1(t)p_2(t+\tau)} &= \sum_n \sum_{n'} \overline{a_n a_{n'}' S_n(t-\tau_n) S_{n'}(t-\tau_{n'}'+\tau)} \\ &= \sum_n a_n a_n' \overline{S_n(t-\tau_n)S_n(t-\tau_n'+\tau)} \\ &= \sum_n a_n a_n' \phi_{S_n}(\tau_n'-\tau_n-\tau)\end{aligned} \tag{13}$$

where $\phi_{S_n}(\tau)$ is the autocorrelation function of sound wave from the n-th source. Now $C(f, 1, 2)$ is written as

$$C(f, 1, 2) = \sum_n a_n a_n' \int_{-\infty}^{\infty} \phi_{S_n}(\tau_n'-\tau_n-\tau) \cos 2\pi f\tau d\tau$$

$$
\begin{aligned}
&= \sum_n a_n a'_n \int_{-\infty}^{\infty} \phi_{S_n}(-\tau) \cos 2\pi f(\tau - \tau_n + \tau'_n) d\tau \\
&= \sum_n a_n a'_n \Big[\int_{-\infty}^{\infty} \phi_{S_n}(\tau) \cos 2\pi f\tau \cos 2\pi f(\tau_n - \tau'_n) d\tau \\
&\quad + \int_{-\infty}^{\infty} \phi_{S_n}(\tau) \sin 2\pi f\tau \sin 2\pi f(\tau_n - \tau'_n) d\tau \Big]
\end{aligned} \tag{14}
$$

Since $\phi_{S_n}(\tau)$ is an even function and $\sin 2\pi f\tau$ is odd, the second term vanishes.

$$
C(f, 1, 2) = \sum_n a_n a'_n \Phi_{S_n}(f) \cos 2\pi f(\tau_n - \tau'_n). \tag{15}
$$

Model experiment is performed in the case of single sound source. Real part of cross power spectrum of noise signal $X(t)$ and its delayed signal $Y(t) = X(t-D)$ is computed by digital electronic spectrum analyzer [3] as shown in Fig. 1 (a). Power spectrum of $X(t)$ and the ratio $C(f)/\Phi_X(f)$ are shown in Fig. 1 (b) and (c). In this case, (15) is reduced to

$$
C(f, X, Y) = a\Phi_X(f) \cos 2\pi fD \tag{16}
$$

which means $C(f)/\Phi_X(f)$ is cosine function as shown in Fig. 1 (c).

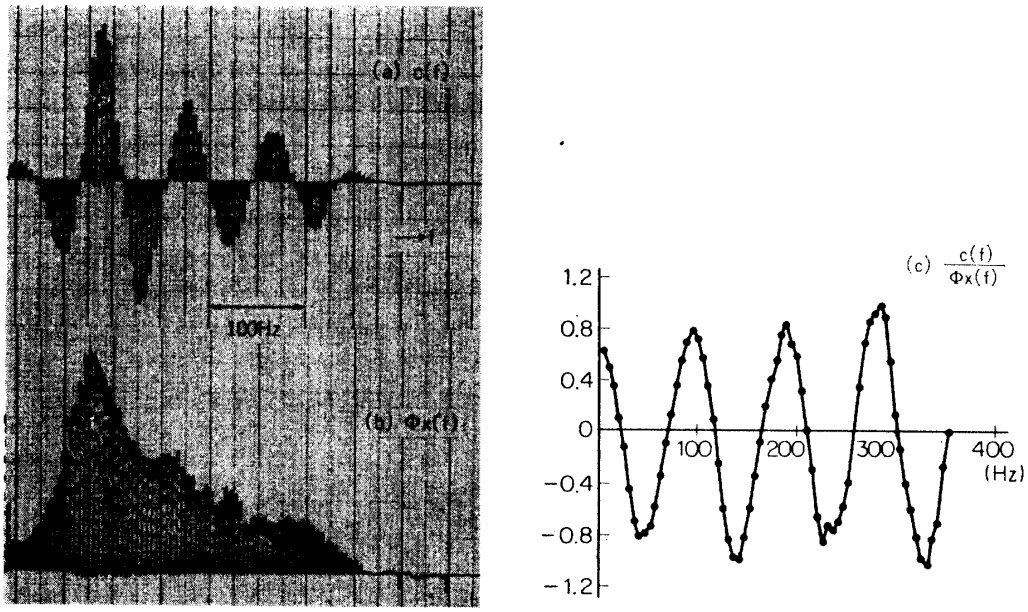

FIG. 1. Example of real part of cross power spectrum.
(a) Real part of cross power spectrum of $X(t)$ and $Y(t) = X(t-D)$. $D = 10.6$ ms.
(b) Power spectrum of $X(t)$.
(c) Ratio of $C(f)$ to $\Phi_X(f)$.
Horizontal axes are in Hz and vertical axes are in arbitrary unit.

3. Generalized Impedance

Generalized impedance $Z_s(i\omega)$ is defined as

$$Z_s(i\omega)=\frac{\mathscr{L}\{L_s(t)\}}{\mathscr{L}\{q_s(t)\}} \tag{17}$$

where $\mathscr{L}\{\ \}$ means Laplace transform. To obtain (17), solution (3) is substituted to system equation (1).

$$\begin{aligned} &L\Big[\sum_s q_s(t)y_s(\boldsymbol{r})\Big]+b\frac{\partial}{\partial t}\Big\{\sum_s q_s(t)y_s(\boldsymbol{r})\Big\} \\ &\quad+\frac{1}{c^2}\frac{\partial^2}{\partial t^2}\Big\{\sum_s q_s(t)y_s(\boldsymbol{r})\Big\}=p(\boldsymbol{r},t) \end{aligned} \tag{18}$$

Since $L[\ \ ]$ is linear operator,

$$\sum_s q_s(t)L[y_s(\boldsymbol{r})]+\sum_s b\,y_s(\boldsymbol{r})\dot{q}_s(t)+\sum_s\frac{1}{c^2}y_s(\boldsymbol{r})\ddot{q}_s(t)=p(\boldsymbol{r},t) \tag{19}$$

From (19) and (2),

$$\sum_s\frac{\omega_s^2}{c^2}q_s(t)y_s(\boldsymbol{r})+\sum_s b\,\dot{q}_s(t)y_s(\boldsymbol{r})+\sum_s\frac{1}{c^2}\ddot{q}_s(t)y_s(\boldsymbol{r})=p(\boldsymbol{r},t) \tag{20}$$

Multiplying both side of (20) by $y_s(\boldsymbol{r})$ and integrate all over the surface,

$$\frac{1}{c^2}\ddot{q}_s(t)+b\dot{q}_s(t)+\frac{\omega_s^2}{c^2}q_s(t)=L_s(t) \tag{21}$$

in which orthonormality of modes are considered.
Laplace transform of (21) is

$$\frac{s^2}{c^2}\mathscr{L}\{q_s(t)\}+bs\mathscr{L}\{q_s(t)\}+\frac{\omega_s^2}{c^2}\mathscr{L}\{q_s(t)\}=\mathscr{L}\{L_s(t)\} \tag{22}$$

$$\therefore\quad Z_s(s)=\frac{\mathscr{L}\{L_s(t)\}}{\mathscr{L}\{q_s(t)\}}=\frac{s^2}{c^2}+bs+\frac{\omega_s^2}{c^2} \tag{23}$$

$$\therefore\quad Z_s(i\omega)=\frac{\omega_s^2}{c^2}-\frac{\omega^2}{c^2}+ib\omega \tag{24}$$

4. Measurement of Generalized Coordinate Variables and Mode Shapes

In the above discussions, vibration magnitude of each mode and effective pressure load to build up that specified mode are considered. In this section, measuring methods of mode shapes and magnitudes will be discussed. First, next quantity is considered.

$$q_{n\epsilon}(t)=\int \xi(\boldsymbol{r},t)y_{n\epsilon}(\boldsymbol{r})dA=\sum_s q_s(t)\int y_s(\boldsymbol{r})y_{n\epsilon}(\boldsymbol{r})dA \tag{25}$$

where $y_{n\epsilon}(\boldsymbol{r})$ is a test function of weighting, which is assumed to be normalized as

$$\int y_{n\epsilon}^2(\boldsymbol{r})dA=1 \tag{26}$$

When damping of the structure b in the equation (24) is small, generalized impedance becomes small when $\omega=\omega_s$, and $\Phi_{q_s}(f)$ shows sharp peak at this resonant frequency ω_s, if $\Phi_{L_s}(f)$ covers this frequency.

Then power spectrum of (25), $\Phi_{q_{n\epsilon}}(f)$ consists a few number of peaks on the frequency axis, whose magnitudes equal to

$$\overline{q_s^2(t)}\left\{\int y_s(\boldsymbol{r})y_{n\epsilon}(\boldsymbol{r})dA\right\}^2.$$

When $y_{n\epsilon}(\boldsymbol{r})=y_n(\boldsymbol{r})$, from orthonormality of modes, the n-th peak shows its maximum value $\overline{q_n^2(t)}$ and other peaks vanish. If we can adjust weight of integration so as to make the n-th peak highest and others disappear, we get both mode shape $y_n(\boldsymbol{r})$ and its magnitude $\overline{q_n^2(t)}$.

In practice, vibration quantity is measured at finite measuring points. They form vector as

$$\boldsymbol{\xi}=\begin{bmatrix}\xi(x_1,t)\\ \vdots\\ \xi(x_k,t)\end{bmatrix}=\sum_s q_s(t)\begin{bmatrix}y_s(x_1)\\ \vdots\\ y_s(x_k)\end{bmatrix}=\sum_s q_s(t)\boldsymbol{y}_s \tag{27}$$

where k is the number of measuring points and measurements are made simultaneously. Weight function also forms k-dimensional vector

$$\boldsymbol{y}'_{n\epsilon}=[y_{n\epsilon 1},\cdots,y_{n\epsilon k}] \tag{28}$$

where prime means transpose. Then $y_s(\boldsymbol{r})$ and $y_{n\epsilon}(\boldsymbol{r})$ in (25) are replaced by vector $\boldsymbol{y}_s$ and $\boldsymbol{y}_{n\epsilon}$.

$$q_{n\epsilon}(t)=\sum_s q_s(t)\boldsymbol{y}'_s\boldsymbol{y}_{n\epsilon}=q_n(t)\boldsymbol{y}'_n\boldsymbol{y}_{n\epsilon}+\sum_{s\neq n} q_s(t)\boldsymbol{y}'_s\boldsymbol{y}_{n\epsilon} \tag{29}$$

Since $\boldsymbol{y}_s$ consists of finite number of sampling values of $y_s(\boldsymbol{r})$, orthonormality of $\{\boldsymbol{y}_s\}$ would be incomplete, but when sampling number is sufficiently large, orthonormality would be correct approximately and above expression stands. Then if $\boldsymbol{y}_{n\epsilon}$ is made to be equal to $\boldsymbol{y}_n$, the first term of (29) becomes maximum and others almost zero.

For that purpose, components of $\boldsymbol{y}_{n\epsilon}$ are adjusted one by one as follows. $\boldsymbol{y}_{n\epsilon i}$ is assumed to be k-dimensional vector whose first i components are parallel to those of $\boldsymbol{y}_n$, and other components are zero. Then the $(i+1)$-th component of $\boldsymbol{y}_{n\epsilon}$ is determined as to make

$$\overline{q_n^2(t)}\,\frac{(\boldsymbol{y}'_n\boldsymbol{y}_{n\epsilon i+1})^2}{\boldsymbol{y}'_{n\epsilon i+1}\boldsymbol{y}_{n\epsilon i+1}} \tag{30}$$

maximum, which makes the first $i+1$ components of $y_{n\varepsilon i+1}$ parallel to those of y_n. Continueing this process $k-1$ times, starting with arbitrary value of first component, $y_{n\varepsilon}$ can be made to be parallel to y_n, and normalization can be made if necessary.

To do these processes, real time spectrum analyzer is very adequate to make (30) maximum by adjusting the weight of summation, for $\overline{q_n^2(t)}\,(y_n' y_{n\varepsilon i+1})^2$ is the magnitude of the n-th spectral peak.

5. Experiments

Measurement of thin structure vibration by strain gage is considered. Surface elongation is expressed as

$$\frac{l+\Delta l}{\rho+h/2}=\frac{l}{\rho} \tag{31}$$

where ρ is radius of curvature and h is thickness of structure as Fig. 2 shows. On the other hand, radius of curvature is expressed by transverse displacement ξ as

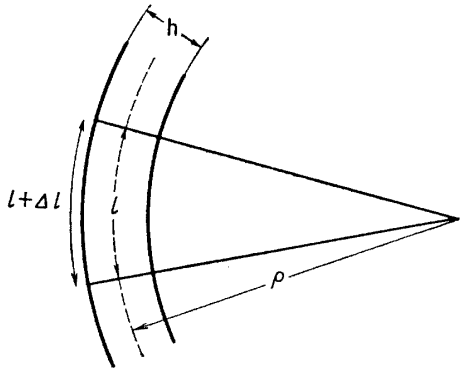

Fig. 2. Relation of radius of curvature ρ and surface elongation Δl.

$$\frac{1}{\rho}=\frac{d^2\xi}{dx^2}\left\{1+\left(\frac{d\xi}{dx}\right)^2\right\}^{-3/2} \tag{32}$$

where x-axis is taken in the direction of strain gage. From (31) and (32), assuming $(d\xi/dx)^2 \ll 1$,

$$\frac{\Delta l}{l}=\frac{h}{2}\frac{d^2\xi}{dx^2} \tag{33}$$

(33) shows that the output signal of strain gage is proportional to the second order differentiation of displacement by space variable.

As a simple example, one dimensional clamped-free beam will be considered in the following. For bending motion of uniform beam whose length is l, mass per unit length is m, area moment of inertia is I and Young's modulus is E, (2) reduces to

$$\frac{d^4y(x)}{dx^4}-\beta^4 y(x)=0, \qquad \beta^4=\frac{\omega^2 m}{EI} \tag{34}$$

where $y(x)$ can be not only displacement variable but also its first, second or third space differentiation, though boundary conditions are different forms for each case. This assures that the twice differentiation of mode function which is measured by strain gage can take place the mode as discussed in the preceding chapters. In fact, set of twice space differentiated functions of modes of this case are shown to be orthogonal by simple calculation as follows.

$$\begin{aligned}\int_0^l \frac{d^2y_s(x)}{dx^2}\frac{d^2y_r(x)}{dx^2}dx &= \left[\frac{d^2y_s(x)}{dx^2}\frac{dy_r(x)}{dx}\right]_0^l - \int_0^l \frac{d^3y_s(x)}{dx^3}\frac{dy_r(x)}{dx}dx \\ &= \left[\frac{d^2y_s(x)}{dx^2}\frac{dy_r(x)}{dx}\right]_0^l - \left[\frac{d^3y_s(x)}{dx^3}y_r(x)\right]_0^l + \int_0^l \frac{d^4y_s(x)}{dx^4}y_r(x)dx\end{aligned} \tag{35}$$

Since the boundary conditions of clamped-free beam are

$$\left.\begin{aligned} y_s(0)&=0 & \left.\frac{dy_s(x)}{dx}\right|_{x=0}&=0 \\ \left.\frac{d^2y_s(x)}{dx^2}\right|_{x=l}&=0 & \left.\frac{d^3y_s(x)}{dx^3}\right|_{x=l}&=0\end{aligned}\right\} \tag{36}$$

the first and second terms of (35) vanish. Then if $s \neq r$,

$$\int_0^l \frac{d^2y_s(x)}{dx^2}\frac{d^2y_r(x)}{dx^2}dx = \int_0^l \frac{d^4y_s(x)}{dx^4}y_r(x)dx = \beta_s^4\int_0^l y_s(x)y_r(x) = 0 \tag{37}$$

Thus the set of functions $\{d^2y_s(x)/dx^2\}$ makes orthogonal set when $\{y_s(x)\}$ is orthogonal. Furthermore in this special case there is more intimate relation between $\{d^2y_s(x)/dx^2\}$ and $\{y_s(x)\}$. Let

$$z_s(x) = \frac{1}{\beta_s^2}\frac{d^2}{dx^2}y_s(l-x) \tag{38}$$

then $z_s(x)$ is shown to satisfy (34) and (36) as

$$\begin{aligned}\frac{d^4z_s(x)}{dx^4} - \beta_s^4 z_s(x) &= \frac{1}{\beta_s^2}\frac{d^6}{dx^6}y_s(l-x) - \beta_s^2\frac{d^2}{dx^2}y_s(l-x) \\ &= \frac{1}{\beta_s^2}\frac{d^2}{dx^2}\beta_s^4 y_s(l-x) - \beta_s^2\frac{d^2}{dx^2}y_s(l-x) = 0\end{aligned} \tag{39}$$

$$z_s(0) = \frac{1}{\beta_s^2}\frac{d^2}{dx^2}y_s(x)\Big|_{x=l} = 0 \tag{40}$$

$$\left.\frac{dz_s(x)}{dx}\right|_{x=0} = \frac{1}{\beta_s^2}\left.\frac{d^3}{dx^3}y_s(l-x)\right|_{x=0} = -\frac{1}{\beta_s^2}\left.\frac{d^3y_s(x)}{dx^3}\right|_{x=l} = 0 \tag{41}$$

$$\left.\frac{d^2z_s(x)}{dx^2}\right|_{x=l} = \frac{1}{\beta_s^2}\left.\frac{d^4}{dx^4}y_s(l-x)\right|_{x=l} = \beta_s^2 y_s(l-x)\Big|_{x=l} = 0 \tag{42}$$

$$\left.\frac{d^3 z_s(x)}{dx^3}\right|_{x=l} = \frac{1}{\beta_s^2}\left.\frac{d^5}{dx^5} y_s(l-x)\right|_{x=l} = \beta_s^2 \left.\frac{d}{dx} y_s(l-x)\right|_{x=l} = 0 \tag{43}$$

Now by the uniqueness of solution of homogeneous differential equation,

$$z_s(x) = C y_s(x) \tag{44}$$

Explicit form of $y_s(x)$ is

$$\begin{aligned} y_s(x) = &(\sin \beta_s l - \sinh \beta_s l)(\sin \beta_s x - \sinh \beta_s x) \\ &+ (\cos \beta_s l + \cosh \beta_s l)(\cos \beta_s x - \cosh \beta_s x) \end{aligned} \tag{45}$$

where

$$\cos \beta_s l \cosh \beta_s l = -1 \tag{46}$$

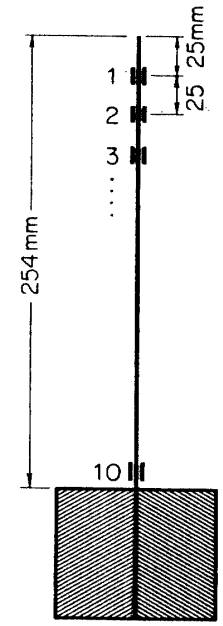

FIG. 3. Clamped-free beam whose length is 254 mm, width 30 mm and thickness 1 mm. Strain gages are attached on both sides at ten points.

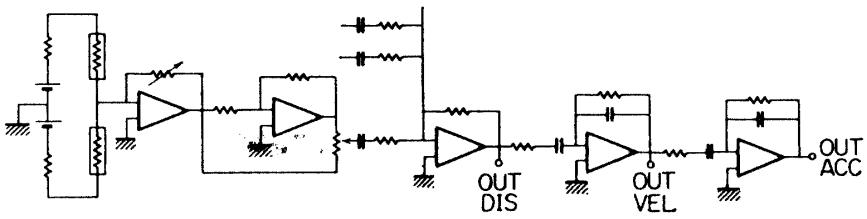

FIG. 4. Strain gages and electronic circuits. Three outputs are available. OUT DIS is for the weighted sum, OUT VEL is for the first order time differentiation of OUT DIS and OUT ACC is for second order time differentiation of OUT DIS.

Vibration of aluminium strip excited by air flow or sound pressure is measured by high sensitivity semiconductor strain gage. Configuration of the test specimen and the electronic circuit are shown in Fig. 3 and 4. Outputs of strain gages are

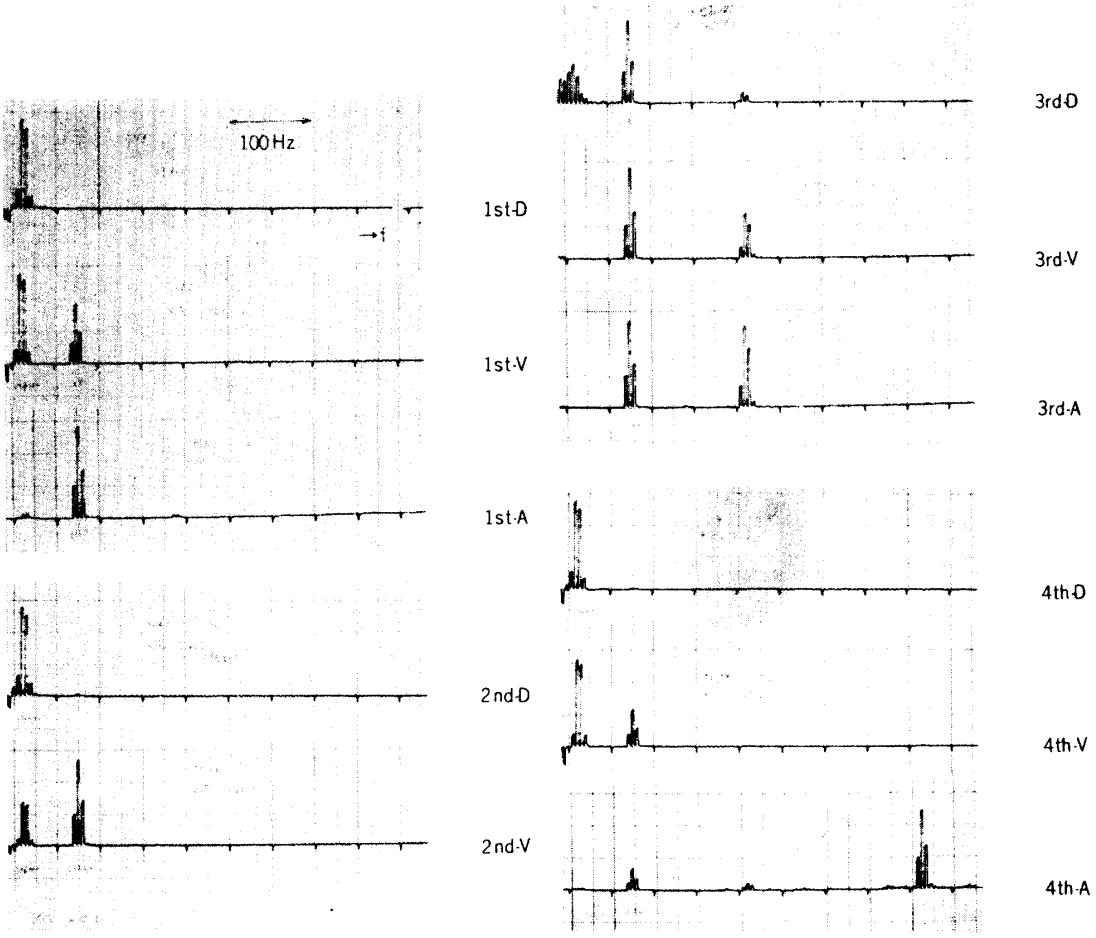

FIG. 5. Power spectra of weighted sum of strain gage outputs when clamped-free beam is excited by air flow. 1st, 2nd, 3rd or 4th means the sort of weighting vector and D, V or A means DIS, VEL or ACC OUT. One step of frequency axis is 5.3 Hz.

summed up with weights which can be adjusted by rotary switches in step-wise. The summed signal is analyzed by a real time spectrum analyzer [3]. Since in many cases low frequency modes are overwhelming, two stages of time differentiating circuits are attached to emphasize high frequency components. Thus three kinds of outputs are available, OUT DIS for original signal, OUT VEL for once differentiated and OUT ACC for twice differentiated signal.

Results of spectrum analysis when the strip is excited by air flow are shown in Fig. 5. The weighting vectors of summation are [5, 4, 4, 3, 2, 2, 1, 1, 0, 0], [5, 3, 0, −2, −3, −4, −4, −3, −2, −1], [5, 1, −2, −4, −2, 0, 3, 4, 3, 1] and [5, 0, −4, −2, 2, 3, 2, −2, −4, −2], which are the quantized values of calculated mode function (second order space differentiated) of 1st, 2nd, 3rd and 4th resonances. For each weighting, three kinds of output, OUT DIS, OUT VEL and OUT ACC are analyzed. Their peak heights are tabulated in Table 1 after necessary corrections. Each column represents four kinds of weightings, and frequencies of observed peaks are in the row. If the weightings are completely equal to the mode shapes, all but diagonal elements would disappear. Three measurements of DIS, VEL and ACC

TABLE 1. Corrected peak heights of Fig. 5

		1st	2nd	3rd	4th
Hz 13.3	D	257,000	191,000	664	95,000
	V	294,000	336,000	—	151,000
	A	—	—	—	—
79.5	D	—	—	1,370	—
	V	6,080	20,200	3,220	2,050
	A	6,110	—	3,140	1,520
225	D	—	—	169	—
	V	—	—	287	—
	A	—	—	99	17
440	D	—	—	—	—
	V	—	—	—	—
	A	—	—	—	66

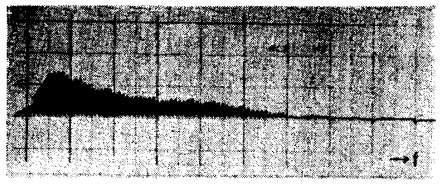

(a)

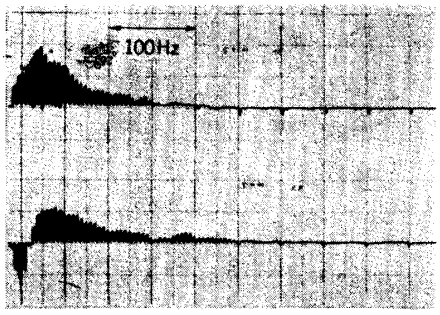

(b-1)

(b-2)

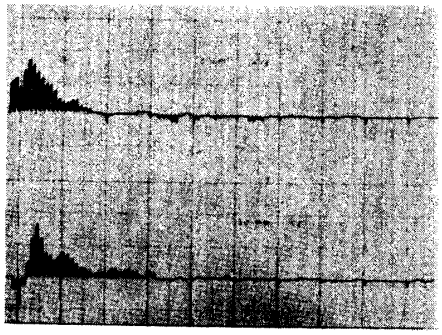

(c-1)

(c-2)

FIG. 6. The power spectrum and the real part of the cross power spectrum of pressure fluctuation in air flow.
(a) Power spectrum detected by 2 mmϕ probe microphone.
(b) Sum of (b-1) and (b-2) is the real part of the cross power spectrum of pressure fluctuation detected at two points separated 5 mm.
(c) Sum of (c-1) and (c-2) is the real part of the cross power spectrum of pressure fluctuation detected at two points separated 20 mm.

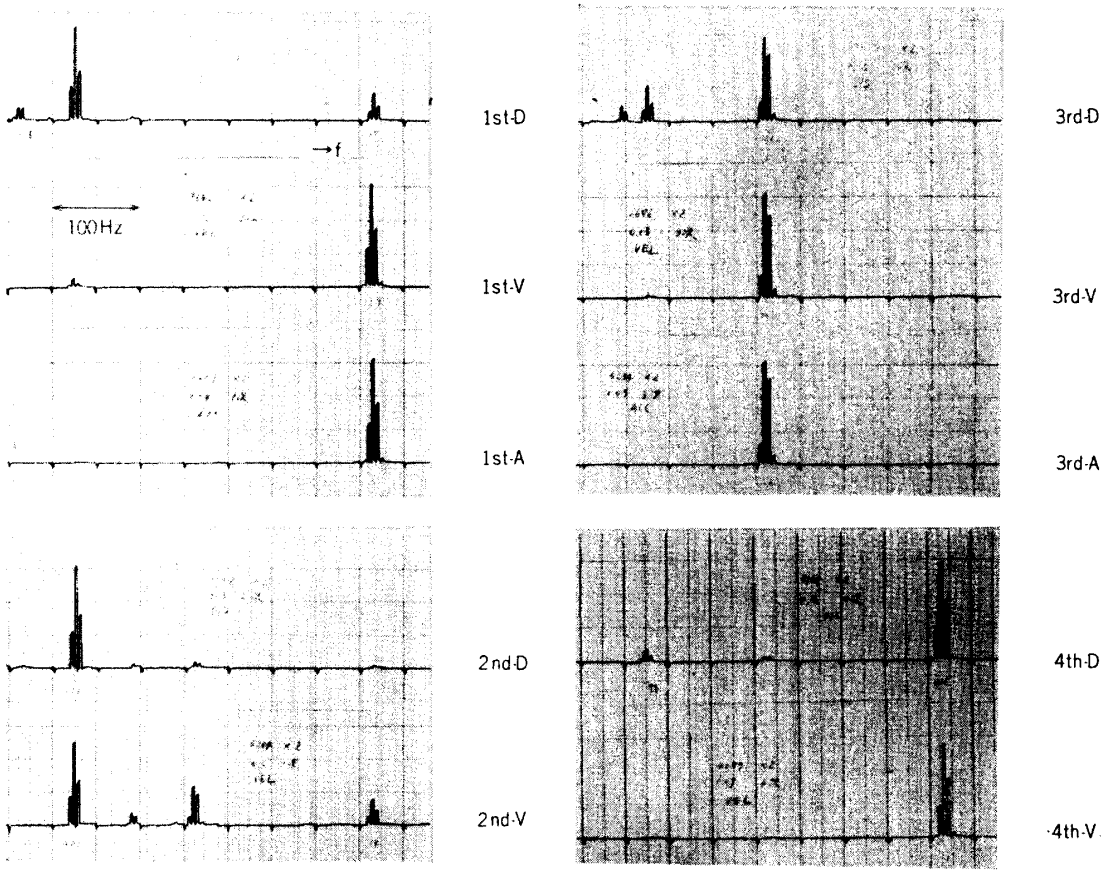

FIG. 7. Power spectra of weighted sum of strain gage outputs when clamped-free beam is excited by sound pressure.

TABLE 2. Corrected peak heights of Fig. 7

		1st	2nd	3rd	4th
Hz 13.3	D	17	—	—	—
	V	—	—	—	—
	A	—	—	—	—
79.5	D	122	851	159	77
	V	131	449	—	—
	A	—	—	—	—
225	D	—	55	364	21
	V	—	38	502	—
	A	—	—	254	—
440	D	35	—	—	606
	V	129	14	—	537
	A	5	—	—	—

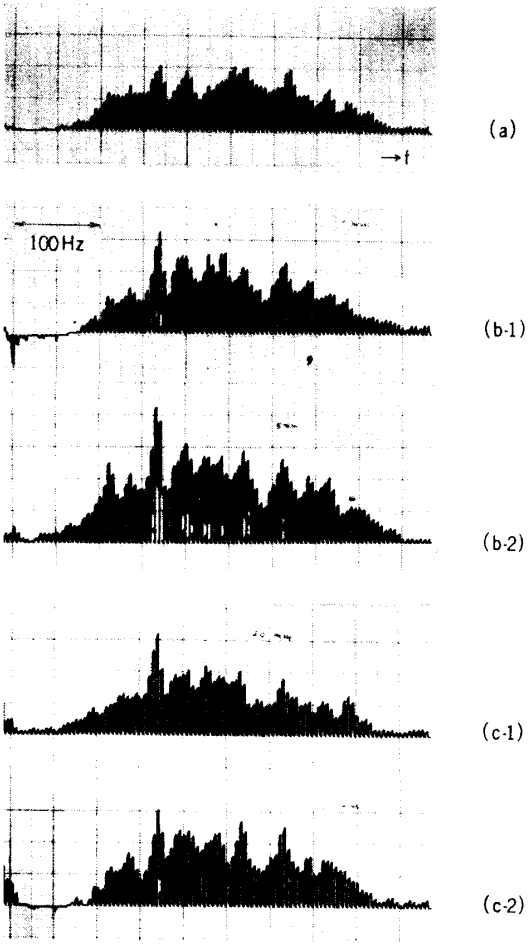

FIG. 8. The power spectrum and the real part of the cross power spectrum of sound pressure.
(a) Power spectrum measured by 1/8 inch condenser microphone.
(b) Sum of (b–1) and (b–2) is the real part of the cross power spectrum of sound field measured at two points separated 5 mm.
(c) Sum of (c–1) and (c–2) is the real part of the cross power spectrum of sound field measured at two points separated 20 mm.

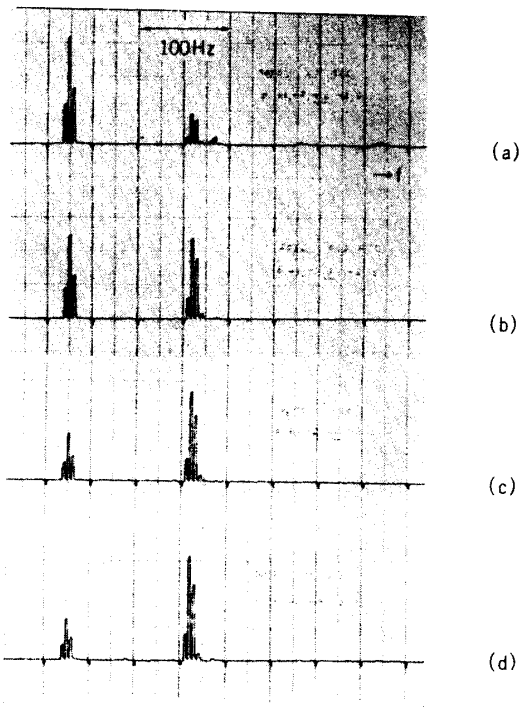

FIG. 9. Power spectra of weighted sum of strain gage outputs when clamped-free beam is excited by air flow. The fourth weight is adjusted to make 225 Hz peak maximum.

should be equal for the same weighting and frequency, but as Table 1 shows, deviation of a few decibels exists, which seems to be caused by unsteadiness of air flow. As a rough estimate, strength of 1st mode is about 15 dB higher than that of 2nd mode, 30 dB higher than 3rd mode and 36 dB higher than 4th mode.

The power spectrum and the real part of the cross power spectrum of pressure fluctuation in air flow are measured by 2 mm$^{\phi}$ probe microphones and shown in Fig. 6. (a) is the power spectrum, (b–1) and (b–2) are the cross power spectra measured by two probes 5 mm separated and (c–1), (c–2) are the cross power spectra measured by two probes 20 mm separated. Since the Fourier transform of

this spectrum analyser is made only positive side, the real part of the cross power spectrum is the sum of (b–1), (b–2) or (c–1), (c–2). (See Appendix)

As the separation of probes increases, the low frequency components of cross spectra become large. (The decrease in extremely low frequency is due to the probe characteristics. Measurements by a hot wire anemometer show that there exists large power in extremely low frequency.) From these facts, the generalized force (10) is estimated to have only low frequency components.

As a second example, the power spectra when clamped-free beam is excited by sound wave are shown in Fig. 7. Beam is placed near the loudspeaker and exposed to 100 dB(C) noise, whose power spectrum and cross power spectra are shown in Fig. 8. Corrected peak heights are shown in Table 2. In this time, strength of 2nd, 3rd and 4th mode are in the same order and 1st mode is almost zero. These are consistent with the power spectrum and cross power spectra of exciting sound pressure shown in Fig. 8.

In Fig. 9, an example of adjusting the weight is illustrated. The beam is excited by air flow and weight of summation is [0, 1, −2, 2, −2, 0, 0, 0, 0, 0] for (a), [0, 1, −2, 0, −2, 0, 0, 0, 0, 0] for (b), [0, 1, −2, −2, −2, 0, 0, 0, 0, 0] for (c) and [0, 1, −2, −4, −2, 0, 0, 0, 0, 0] for (d). Only the fourth weight is varied and when it takes the value −4, the peak at 225 Hz grows to be maximum.

6. Conclusions

Vibration analysis using power spectrum of generalized coordinate is performed. Since the calculation of generalized force (10) is difficult, estimation of vibration strength from exciting force is not attempted. Analyzing the weighted sum of strain gage outputs, it is shown that the measurement of mode shape and vibration strength is possible for simple cases.

The author wishes to express his great thanks to Professor Juichi Igarashi and Dr. Yasushi Ishii for their valuable advices and encouragements.

Department of Instrument and Electronics
Institute of Space and Aeronautical Science
University of Tokyo, Tokyo
May 20, 1970

References

[1] Leonard Meirovitch: Analytical Methods in Vibration, Macmillan, 1967.
[2] B. L. Clarkson: Technical Aspects of Sound, Vol. 3, Chap. 4 (ed. by Richardson and Meyer), Elsevier, 1962.
[3] Yasushi Ishii: A Real-Time Signal Processing System for Correlation and Spectrum Analysis, Report of the Institute of Space and Aeronautical Science, University of Tokyo, No. 444, February 1970.

APPENDIX

Real part of the cross power spectrum of $x(t)$ and $y(t)$ is given as

$$C(f)=\int_{-\infty}^{\infty}\overline{x(t)y(t+\tau)}\cos 2\pi f\tau d\tau$$

On the other hand, the spectrum analyzer used in this study performs next operation.

$$\int_{0}^{T}\overline{x(t)y(t+\tau)}\cos 2\pi f\tau d\tau$$

When power spectrum is measured, which means $x(t)=y(t)$, autocorrelation function is even function of τ, so two times of above equation equals the power spectrum function, if the autocorrelation can be considered zero outside the region $-T<\tau<T$. When cross spectrum is considered, cross correlation function is not even function, so some techniques must be used. $C(f)$ is rewritten as

$$\begin{aligned}C(f)&=\int_{0}^{\infty}\overline{x(t)y(t+\tau)}\cos 2\pi f\tau d\tau+\int_{-\infty}^{0}\overline{x(t)y(t+\tau)}\cos 2\pi f\tau d\tau\\&=\int_{0}^{\infty}\overline{x(t)y(t+\tau)}\cos 2\pi f\tau d\tau+\int_{0}^{\infty}\overline{x(t)y(t-\tau)}\cos 2\pi f\tau d\tau\end{aligned}$$

Replacing $x(t)\rightarrow y'(t)$, $y(t)\rightarrow x'(t)$

$$\begin{aligned}C(f)&=\int_{0}^{\infty}\overline{x(t)y(t+\tau)}\cos 2\pi f\tau d\tau+\int_{0}^{\infty}\overline{x'(t-\tau)y'(t)}\cos 2\pi f\tau d\tau\\&=\int_{0}^{\infty}\overline{x(t)y(t+\tau)}\cos 2\pi f\tau d\tau+\int_{0}^{\infty}\overline{x'(t)y'(t+\tau)}\cos 2\pi f\tau d\tau\end{aligned}$$

This means by changing input terminals of spectrum analyzer and making two measurements, real part of the cross power spectrum can be measured as a sum of them. When the cross correlation function is restricted only in the positive side, as in the case of Fig. 1, the measurement is enough for one time.